Circulation Research

ORIGINAL RESEARCH

# Rewiring Endothelial Sphingolipid Metabolism to Favor S1P Over Ceramide Protects From Coronary Atherosclerosis

Onorina L. Manzo, Jasmine Nour, Linda Sasset, Alice Marino, Luisa Rubinelli, Sailesh Palikhe, Martina Smimmo, Yang Hu, Maria Rosaria Bucci, Alain Borczuk, Olivier Elemento, Julie K. Freed, Giuseppe Danilo Norata, Annarita Di Lorenzo

**BACKGROUND:** Growing evidence correlated changes in bioactive sphingolipids, particularly S1P (sphingosine-1-phosphate) and ceramides, with coronary artery diseases. Furthermore, specific plasma ceramide species can predict major cardiovascular events. Dysfunction of the endothelium lining lesion-prone areas plays a pivotal role in atherosclerosis. Yet, how sphingolipid metabolism and signaling change and contribute to endothelial dysfunction and atherosclerosis remain poorly understood.

**METHODS:** We used an established model of coronary atherosclerosis in mice, combined with sphingolipidomics, RNA-sequencing, flow cytometry, and immunostaining to investigate the contribution of sphingolipid metabolism and signaling to endothelial cell (EC) activation and dysfunction.

**RESULTS:** We demonstrated that hemodynamic stress induced an early metabolic rewiring towards endothelial sphingolipid de novo biosynthesis, favoring S1P signaling over ceramides as a protective response. This finding is a paradigm shift from the current belief that ceramide accrual contributes to endothelial dysfunction. The enzyme SPT (serine palmitoyltransferase) commences de novo biosynthesis of sphingolipids and is inhibited by NOGO-B (reticulon-4B), an ER membrane protein. Here, we showed that NOGO-B is upregulated by hemodynamic stress in myocardial EC of ApoE$^{-/-}$ mice and is expressed in the endothelium lining coronary lesions in mice and humans. We demonstrated that mice lacking NOGO-B specifically in EC (Nogo-A/B$^{ECKO}$ApoE$^{-/-}$) were resistant to coronary atherosclerosis development and progression, and mortality. Fibrous cap thickness was significantly increased in Nogo-A/B$^{ECKO}$ApoE$^{-/-}$ mice and correlated with reduced necrotic core and macrophage infiltration. Mechanistically, the deletion of NOGO-B in EC sustained the rewiring of sphingolipid metabolism towards S1P, imparting an atheroprotective endothelial transcriptional signature.

**CONCLUSIONS:** These data demonstrated that hemodynamic stress induced a protective rewiring of sphingolipid metabolism, favoring S1P over ceramide. NOGO-B deletion sustained the rewiring of sphingolipid metabolism toward S1P protecting EC from activation under hemodynamic stress and refraining coronary atherosclerosis. These findings also set forth the foundation for sphingolipid-based therapeutics to limit atheroprogression.

**GRAPHIC ABSTRACT:** A graphic abstract is available for this article.

**Key Words:** atherosclerosis ■ endothelial cells ■ hemodynamics ■ macrophages ■ sphingolipids

Meet the First Author, see p 953

Endothelial activation and dysfunction are critical events in the initiation and progression of atherosclerosis, resulting in proinflammatory and prothrombotic signaling, dysregulation of vascular tone, and barrier function. These changes further promote the accumulation of inflammatory cells and lipoproteins in the arterial wall.[1–3] Risk factors such as dyslipidemia and hypertension are recognized to set off endothelial dysfunction.[4,5]

Correspondence to: Annarita Di Lorenzo, PhD, Department of Pathology and Laboratory Medicine, Cardiovascular Research Institute, Feil Brain and Mind Research Institute, Weill Cornell Medical College, 1300 York Ave, New York, NY 10021. Email and2039@med.cornell.edu
Supplemental Material is available at https://www.ahajournals.org/doi/suppl/10.1161/CIRCRESAHA.123.323826.
For Sources of Funding and Disclosures, see page 1003.

*Circulation Research* is available at www.ahajournals.org/journal/res

## Novelty and Significance

### What Is Known?

- Plasmatic levels of sphingolipid ceramides can predict major cardiovascular events and are elevated in patients affected by coronary artery diseases (CAD).
- Circulating levels of S1P (sphingosine-1-phosphate), a lipid beneficial for the vasculature, are decreased in patients with CAD.
- The Nogo-B protein downregulates de novo biosynthesis of sphingolipids, including ceramides and S1P, and genome-wide association studies show association of a reticulon-4 gene variant (Nogo proteins) with CAD.

### What New Information Does This Article Contribute?

- Ceramide levels are not increased in endothelial cells (EC) of mice affected by coronary atherosclerosis.
- Nogo-B deletion in EC promotes a metabolic shift toward S1P signaling, without affecting ceramide levels.
- The loss of Nogo-B protects EC from activation and dysfunction, reduces inflammation, and coronary atherosclerosis formation and progression.

Plasma levels of ceramide and S1P, 2 major bioactive sphingolipids, change in patients affected by cardiovascular diseases. While S1P decreases in patients affected by CAD, specific ceramides can predict major cardiovascular events.

Endothelial dysfunction is an early and paramount event in atherosclerosis. Whether changes in sphingolipids, particularly ceramide and S1P, occur in the endothelium in vivo and contribute to atherogenesis is unknown. This is particularly significant considering that this pathway is amenable to therapeutics.

Nogo-B protein can downregulate the de novo production of sphingolipids and a genetic study correlated a variant of reticulon-4 gene (Nogo) with CAD, but the underlying mechanisms remain poorly understood. Our studies using a novel mouse model of coronary atherosclerosis show that Nogo-B contributes to endothelial activation, and atherosclerosis. The loss of Nogo-B in EC promotes a metabolic shift toward S1P without affecting ceramides. Rewiring of metabolism in favor of S1P protects the EC from activation under stress conditions and restrains coronary atherosclerosis development and progression.

## Nonstandard Abbreviations and Acronyms

| | |
|---|---|
| **CAD** | coronary artery disease |
| **CD206** | cluster differentiation 206 |
| **dhSph-1P** | dihydrosphingosine-1-phosphate |
| **EC** | endothelial cell |
| **LAD** | left anterior descending |
| **S1P** | sphingosine-1-phosphate |
| **S1PR1** | S1P receptor 1 |
| **SMC** | smooth muscle cell |
| **Spns2** | spinster-2 |
| **SPT** | serine palmitoyltransferase |
| **SPTLC1** | serine palmitoyltransferase long chain base subunit 1 |
| **SPTLC2** | serine palmitoyltransferase long chain base subunit 2 |
| **TAC** | transverse aortic constriction |

Yet, targeting endothelial cells (EC) in inflammatory diseases, such as atherosclerosis, remains a challenge.

Low-density lipoproteins are key to atherosclerosis and represent the therapeutic target of cholesterol-lowering drugs.[6,7] Nevertheless, emerging studies demonstrate a strong correlation between plasma sphingolipid ceramide levels, in particular C16:0-, C18:0-, and C24:1-ceramides, and the incidence of major adverse cardiovascular events,[8–10] which is independent of other classical risk factors such as cholesterol, hypertension, and diabetes. Some plasma ceramides can also predict major cardiovascular events in patients with coronary artery disease (CAD)[10,11] and patients affected by familial CAD present higher plasma ceramides and other sphingolipids levels compared with healthy controls.[12] Interestingly, contrary to ceramides, S1P (sphingosine-1-phosphate), a bioactive lipid exerting beneficial cardiovascular functions is decreased in patients with CAD,[13,14] suggesting that a dysregulation of sphingolipid metabolism and signaling can underlie these conditions.

S1P and ceramides are both bioactive lipids and are considered to have beneficial and deleterious effects on the vasculature, respectively.[8,15,16] Ceramides are elevated in cultured EC exposed to TNFα (tumor necrosis factor alpha), high glucose, or high glucose/palmitate.[8] Elevated ceramides decrease NO bioavailability via PP2A (protein phosphatase 2A)-mediated endothelial nitric oxide synthase[17] dephosphorylation[18] and reactive oxygen species (ROS) formation.[19] Therefore, ceramides have been suggested to contribute to endothelial dysfunction. However, whether ceramide accrual occurs in EC in vivo and contributes to dysfunction has never been demonstrated.

As cholesterol, ceramides are elevated in atherosclerotic lesions.[20] The deletion of both, *Sptlc1* or *Sptlc2* gene,

coding the 2 subunits of SPT (serine palmitoyltransferase), is embryonically lethal[21]; and selective deletion of *Sptlc2* in cardiomyocytes causes dilated cardiomyopathy,[22] suggesting that SPT function is necessary for survival and health.

Myriocin treatment, a drug inhibiting the enzyme SPT, and hence ceramides and S1P, reduces atherosclerosis.[23,24] However, in addition to reducing systemic sphingolipids, myriocin lowers both cholesterol and triglycerides and shows immunosuppressive actions,[25] suggesting atheroprotective effects potentially related to arterial wall, lipoprotein, and immune cell mechanisms.[26]

Another unwanted effect of myriocin is the decrease of S1P,[23] a potent activator of eNOS (endothelial nitric oxide synthase)[17] via S1PR1 (S1P receptor 1), which regulates blood flow and pressure.[27] S1P signaling also enhances the endothelial barrier and suppresses inflammation.[28] Furthermore, endothelial *S1pr1* knockout mice are hypertensive[27] and prone to atherosclerosis[29] supporting the vasculoprotective role of this lipid and arguing against a systemic suppression of sphingolipid biosynthesis by myriocin, especially in the vascular wall.

Therefore, understanding how atherosclerotic risk factors impact sphingolipid metabolism and signaling in vivo is of paramount importance to understand the pathogenetic role of these lipids and how they can be therapeutically targeted to reinstate vascular homeostasis.

We discovered that NOGO-B (reticulon-4B), a membrane protein of the endoplasmic reticulum highly expressed in the vascular wall, downregulates SPT activity, thereby controlling sphingolipid production, particularly endothelial S1P. NOGO-B inhibition of SPT activity results in inflammation,[30,31] hypertension,[32] and cardiac hypertrophy.[31]

Few studies have correlated NOGO proteins with CAD. SNP in *Rtn4* gene codifying for NOGO proteins was significantly associated with CAD,[33] while NOGO expression was reported in atherosclerotic lesions.[34,35] However, how sphingolipid metabolism within the vascular wall, especially in the endothelium, changes and contributes to coronary atherosclerosis has never been studied. Recently, we showed that ApoE$^{-/-}$ mice subjected to transverse aortic constriction[36] can develop atherosclerotic lesions in coronary arteries on a chow diet, with characteristics that recapitulate human conditions.[36]

By using this model, we demonstrated that hemodynamic stress in vivo triggers a systematic shift in endothelial sphingolipid metabolism favoring S1P over ceramides. In this setting, the boost in sphingolipid de novo biosynthesis is matched by increased ceramides degradation, resulting in elevated sphingosine and S1P generation. This metabolic shift favoring S1P over ceramides appeared to be a transient protective response of the endothelium to hemodynamic stress, which if sustained could be atheroprotective, and the genetic approach in mice corroborated this hypothesis. The loss of NOGO-B protected EC from activation and dysfunction, by enhancing the metabolic shift towards S1P signaling, without affecting ceramide levels. These findings question the accrual of ceramides as a causal event of endothelial dysfunction and atherosclerosis. In summary, this study discovered that *Nogo-B* deletion can sustain the rewiring of sphingolipid metabolism toward S1P protecting EC from activation under hemodynamic stress and refraining coronary atherosclerosis development and progression.

# METHODS

## Data Availability

A detailed description of all material and methods can be found in the Supplemental Methods and the tables in the Supplemental Material. The data that support the findings of this findings are available upon reasonable request.

## Ethic Statements

The animal studies were reviewed and approved by the Institutional Animal Care and Use Committee of the Weill Cornell Medicine of Cornell University.

# RESULTS

## NOGO-B Is Expressed in the Endothelium of Coronary Plaques in Human and Mice

Hematoxylin and eosin (H&E) staining of human coronary arteries with moderate (Figure 1A) and severe (Figure 1B) atherosclerotic lesions showed the overall structure of the plaques, highlighting the fibrous cap (FB), the necrotic core and the lumen (L, Figure 1Aa and 1Ba). NOGO-B is the most abundant isoform expressed in the vascular wall.[32,37] Immunofluorescent staining showed NOGO-B expression in EC (Figure S1; Figure 1Ac through 1Ae and 1Ag through IAi); smooth muscle cells (SMCs) of neointima and media of coronary artery (Figure S2A). NOGO-B was also expressed in EC of severe coronary lesions (Figure 1Bc through 1Be and IBg through IBi), suggesting that NOGO-B may play a role in atherosclerosis. However, NOGO-B expression was no different in coronary artery specimens from patients with and without a clinical diagnosis of CAD (Table 1; Figure S2B through S2E). It is noteworthy to mention that in coronary arteries, SMC prevails and most likely contributes to NOGO-B expression of the vascular tissue seen in Western Blot (WB) analysis.

Next, we investigated NOGO-B expression in atherosclerotic plaques of left descending artery (LAD) of ApoE$^{-/-}$ mice[36] at 8 weeks after transverse aortic constriction (TAC, Figure 1C). Oil-red-O/hematoxylin staining evidenced lipid deposition in the LAD (Figure 1Da, 1Df, 1Dk, 1Dp; Figure S3). In healthy LAD, NOGO-B was expressed in EC and SMC (Figure 1Db through 1Dd). In LAD with different degrees of atherosclerosis,

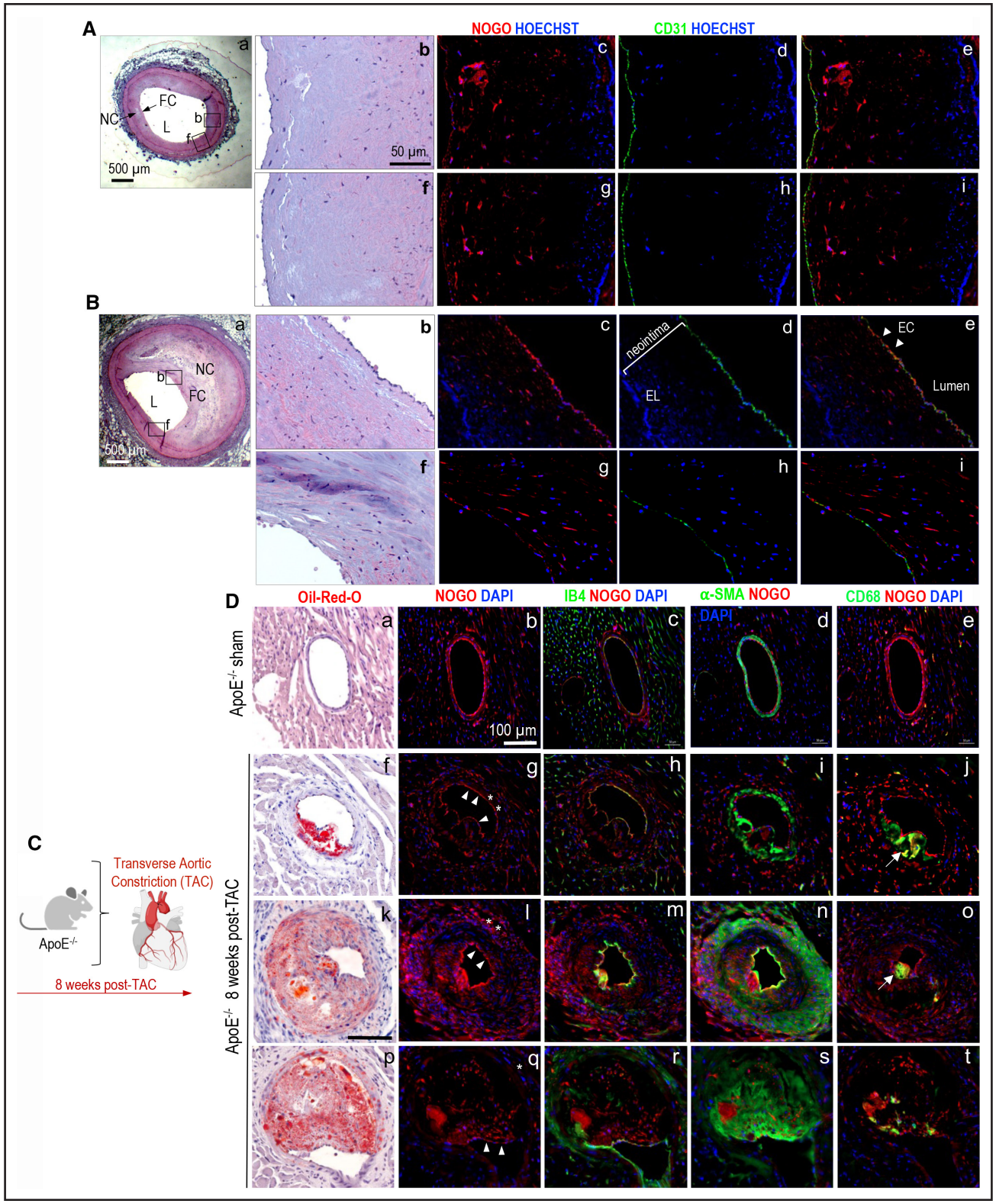


**Figure 1. NOGO-B (reticulon-4B) expression in coronary plaques of humans and mice.**
**A** and **B**, Representative images of immunofluorescence staining for NOGO-B of paraffin sections of human coronary lesions. **Aa**, Hematoxylin and eosin (H&E) staining of human coronary plaque showing the necrotic core (NC) and fibrous cap (FC). **Ab** and **Af**, High magnification of H&E staining and (**Ac–Af** and **Ag**) immunofluorescent staining for NOGO-B in consecutive sections of human coronary lesions in **Aa**. **Ac** through **Ae**, NOGO-B is expressed in endothelial cell (EC) stained for CD31 (green) and some cells of the neointima. **Ba**, H&E staining of human coronary plaque. **Ba** and **Bf**, High magnification of the H&E staining and (**Bc–Bf** and **Bg**) Immunofluorescence staining of CD31+ EC expressing NOGO-B (arrowheads). **C**, Mouse model of coronary atherosclerosis. Male and female ApoE$^{-/-}$ mice were subjected to transverse aortic constriction (TAC) or sham surgery, and 8 weeks later, the hearts were sectioned from the base to the apex to assess atherosclerotic (*Continued*)

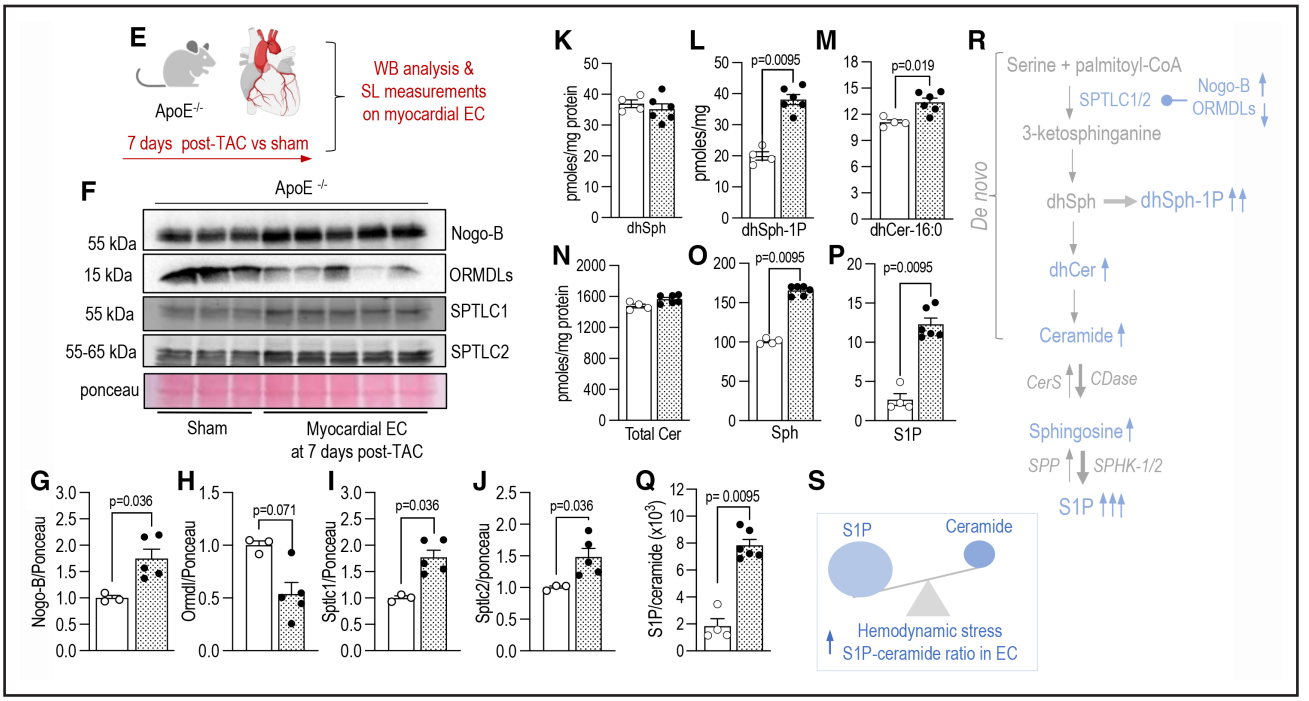


**Figure 1 Continued.** lesions in the left anterior descending (LAD) artery. **D**, Consecutive myocardial sections were stained with oil-red-O/hematoxylin and immunofluorescent antibody against NOGO-B, isolectin B4 (green, marker of EC), α-smooth muscle actin (green, marker of smooth muscle cells), CD68 (green, monocyte/macrophage marker), DAPI (nuclei, blue). Oil-red-O/hematoxylin-stained images show the LAD affected by different degrees of atherosclerosis. Scale bar: 100 µm. **E**, Male and female ApoE$^{-/-}$ mice underwent TAC or sham surgery. After 7 days, Western Blot (WB) analysis and sphingolipid measurements were performed on myocardial EC. **F**, WB analysis and quantification of (**G**) NOGO-B, (**H**) ORMDL2 (orosomucoid 1 like protein), (**I**) SPTLC1 (serine palmitoyltransferase long chain base subunit 1), and (**J**) SPTLC2 (serine palmitoyltransferase long chain base subunit 2) in myocardial EC isolated from 7 days TAC- (n=5) or sham-operated (n=3) mice. Band intensities were normalized to red ponceau. Statistical significance was assessed by Mann-Whitney *U* test. Measurements of (**K**) dihydrosphingosine (dhSph), (**L**) dhSph-1P (dihydrosphingosine-1-phosphate), (**M**) dihydroceramide-16:0 (dhCer-16:0), (**N**) total ceramides, (**O**) Sph, and (**P**) S1P (sphingosine-1-phosphate) in myocardial EC isolated from 7 days TAC- (n=6) or sham-operated (n=3) mice. **Q**, Ratio of S1P/total ceramides. **K** through **Q**, Statistical significance was assessed by using Mann-Whitney *U* test. **R**, Scheme of the de novo sphingolipid pathway representing the changes in sphingolipids. **S**, Schematic representation of S1P/ceramide ratio in EC at 7 days post-TAC vs sham-operated mice. **G** through **J**, **K** through **Q**, Data are expressed as mean±SEM.

immunofluorescent staining showed NOGO-B expression in EC (Figure 1Dc, 1Dh, 1Dm, 1Dr), and macrophage (Figure 1Dj, 1Do, 1Dt; Figure S4). In some SMC of LAD lesions, NOGO-B staining had a trend of decrease compared with controls (Figure 1Dg and 1Dl versus Figure 1Db; asterisks in Figure 1Dg, Figure 1Dl indicate SMC). Next, we assessed whether the pressure overload affected the SPT complex in myocardial EC at 7 days post-TAC (Figure 1E). Interestingly, WB analysis showed that components of the SPT complex were dramatically changed (Figure 1F). Specifically, both SPTLC1 (serine palmitoyltransferase long chain base subunit 1) and SPTLC2 (serine palmitoyltransferase long chain base subunit 2) of SPT were significantly increased (Figure 1I and 1J), suggesting an upregulation of the de novo biosynthesis. However, SPT inhibitors were differentially regulated, with ORMDL (orosomucoid 1 like protein) decreased and NOGO-B increased compared with EC from the control sham (Figure 1G and 1H). Of note, NOGO-B is the main isoform expressed in EC,[32] with NOGO-A undetectable. Sphingolipidomic analysis showed that dh-sphingosine-1P, C16:0-dhCer, sphingosine (downstream metabolite of ceramide), and S1P were all significantly augmented following TAC compared with sham (Figure 1K through 1P). These data indicate that following hemodynamic stress, both endothelial de novo biosynthesis and degradation of ceramides are increased, with a net shift of the ceramide-S1P rheostat toward S1P signaling (Figure 1Q), as protective mechanisms (Figure 1R and 1S).

## Endothelial-Specific Deletion of NOGO-B Protects the Mice From Coronary Atherosclerosis

EC activation plays a key role in atherogenesis.[3] The expression of endothelial adhesion molecules and cytokines/chemokines favors the accumulation of lipoproteins and inflammatory cells into the vascular wall, a crucial step in the development of atherosclerosis.[38–40] To test the hypothesis that NOGO-B contributes to endothelial dysfunction and atherosclerosis, we generated mice lacking *Nogo-B* specifically in EC on ApoE$^{-/-}$ background (Nogo-A/B$^{ECKO}$ApoE$^{-/-}$; Figure 2A).

**Table 1. Demographic Information of the Patients With and Without CAD**

| Patient | Age | Sex | Medical history | Smoking | BMI | Race | Ethnicity |
|---|---|---|---|---|---|---|---|
| Patients without CAD | | | | | | | |
| 11540 | 58 | Male | … | Active smoker | 19.6 | Unknown | Unknown |
| 11879 | 47 | Female | … | Tobacco use | 36.4 | Black | Unknown |
| 14642 | 22 | Male | … | Tobacco use | 22.8 | White | Unknown |
| 12587 | 53 | Male | … | … | Unknown | Unknown | Unknown |
| 12688 | 49 | Male | Hyperlipidemia | Tobacco use | Unknown | White | Unknown |
| 12295 | 60 | Male | Hypertension | Active smoker | 15.7 | Black | Unknown |
| Patients with CAD | | | | | | | |
| 11656 | 47 | Male | Myocardial infarction and hyperlipidemia | Active smoker | 31.9 | White | Unknown |
| 12531 | 61 | Male | Hypertension and diabetes | Active smoker | 38.4 | Black | Unknown |
| 12259 | 74 | Female | Hypertension | … | Unknown | Unknown | Unknown |
| 12266 | 50 | Female | Hypertension and diabetes | … | Unknown | Black | Unknown |
| 13108 | 59 | Male | Congestive heart failure, atrial fibrillation, and diabetes | … | 27.4 | White | Unknown |

Coronary artery specimens from these 2 groups of patients have been analyzed for Western Blot (refer to Figure S2). BMI indicates body mass index; and CAD, coronary artery disease.

In the absence of NOGO-B, FACS (fluorescence-activated cell sorting) analysis showed a significant reduction in VCAM1 (vascular cell adhesion protein 1) in myocardial EC at 7 days post-TAC compared with sham-operated mice (Table S1; Figure 2B through 2D; Figure S5). The expression of EC cytokine/chemokine genes, including Mcp1, Il1β (interleukin-1 beta), and Cxcl2 (Figure 2E through 2G) was also significantly diminished, in line with a reduction of myocardial CD45+ cells infiltration compared with ApoE$^{-/-}$ (Figure 2H and 2I). Altogether, these data support an in vivo proinflammatory role of endothelial NOGO-B.

At 8 weeks post-TAC, histological analysis was performed to map coronary lesions and assess the degree of stenosis and lipid deposition (Figure 2J). Figure 2K shows representative hearts from ApoE$^{-/-}$ mice at 8 weeks post-TAC showing white-colored LAD due to the presence of atherosclerotic lesions compared with sham-operated mice. Representative reconstruction of the LAD from the base to the apex ApoE$^{-/-}$ and Nogo-A/B$^{ECKO}$ApoE$^{-/-}$ hearts are shown in Figure S6. Analysis of LAD lesions (Figure 2L) demonstrated that the occurrence of LAD lesions with stenosis was significantly reduced in Nogo-A/B$^{ECKO}$ApoE$^{-/-}$ (62.5%) versus of ApoE$^{-/-}$ (84.2%) mice (Figure 2M). Of note, to assess the extent of TAC, the ligations were removed from mice postmortem and measured for the area (Figure S7). Furthermore, the LAD stenosis throughout the heart (from the aortic valve to the apex) was significantly reduced in Nogo-A/B$^{ECKO}$ApoE$^{-/-}$ versus ApoE$^{-/-}$ mice (Figure 2N and 2O, and representative images Figure 2P), as well as the oil-red-O staining of the LAD compared with ApoE$^{-/-}$ mice (Figure 2Q and 2R), suggesting that the loss of endothelial NOGO-B protected the mice from the development and progression of atherosclerosis.

Compared with wild type (WT) (C57Bl6/J) mice, plasma cholesterol levels were significantly increased to a similar extent in ApoE$^{-/-}$ and Nogo-A/B$^{ECKO}$ApoE$^{-/-}$ mice (Figure 2S), thus excluding the reduction of lipid accumulation in Nogo-A/B$^{ECKO}$ApoE$^{-/-}$ LAD could be the consequence of improved lipoprotein metabolism.

## The Loss of Endothelial NOGO-B Improved Cardiac Function and Survival Rate

Echocardiographic analysis (Figure 3A) showed a significant decrease in diastolic and systolic left ventricle (LV) internal diameters (Figure 3B and 3C) and preserved fractional shortening (Figure 3D, index of systolic function), in Nogo-A/B$^{ECKO}$ApoE$^{-/-}$ compared with ApoE$^{-/-}$ mice at 6 weeks post-TAC. Furthermore, the survival rate post-TAC was also significantly higher in Nogo-A/B$^{ECKO}$ApoE$^{-/-}$ mice versus controls (Figure 3E), indicating that endothelial NOGO-B deletion protected the mice from heart failure and death.

Plasma sphingolipid profile (Figure 3F through 3O) showed that S1P was significantly reduced in TAC-operated ApoE$^{-/-}$ mice (Figure 3F), similar to the changes occurring in humans affected by CAD.[14] On the contrary, total ceramides were significantly increased in ApoE$^{-/-}$ post-TAC (Figure 3H), similar to the changes reported in patients with CAD.[11] Specifically, C16:0-, C20:0-, and C22:0-ceramides were elevated in ApoE$^{-/-}$ mice post-TAC compared with sham-operated mice (Figure 3I, 3L, and 3N).

Although LAD lesions were markedly reduced in Nogo-A/B$^{ECKO}$ApoE$^{-/-}$, there were no differences in ceramide and S1P plasma levels between the 2 genotypes (Figure 3F through 3N), suggesting that plasma sphingolipids did not correlate with severity of the

ORIGINAL RESEARCH

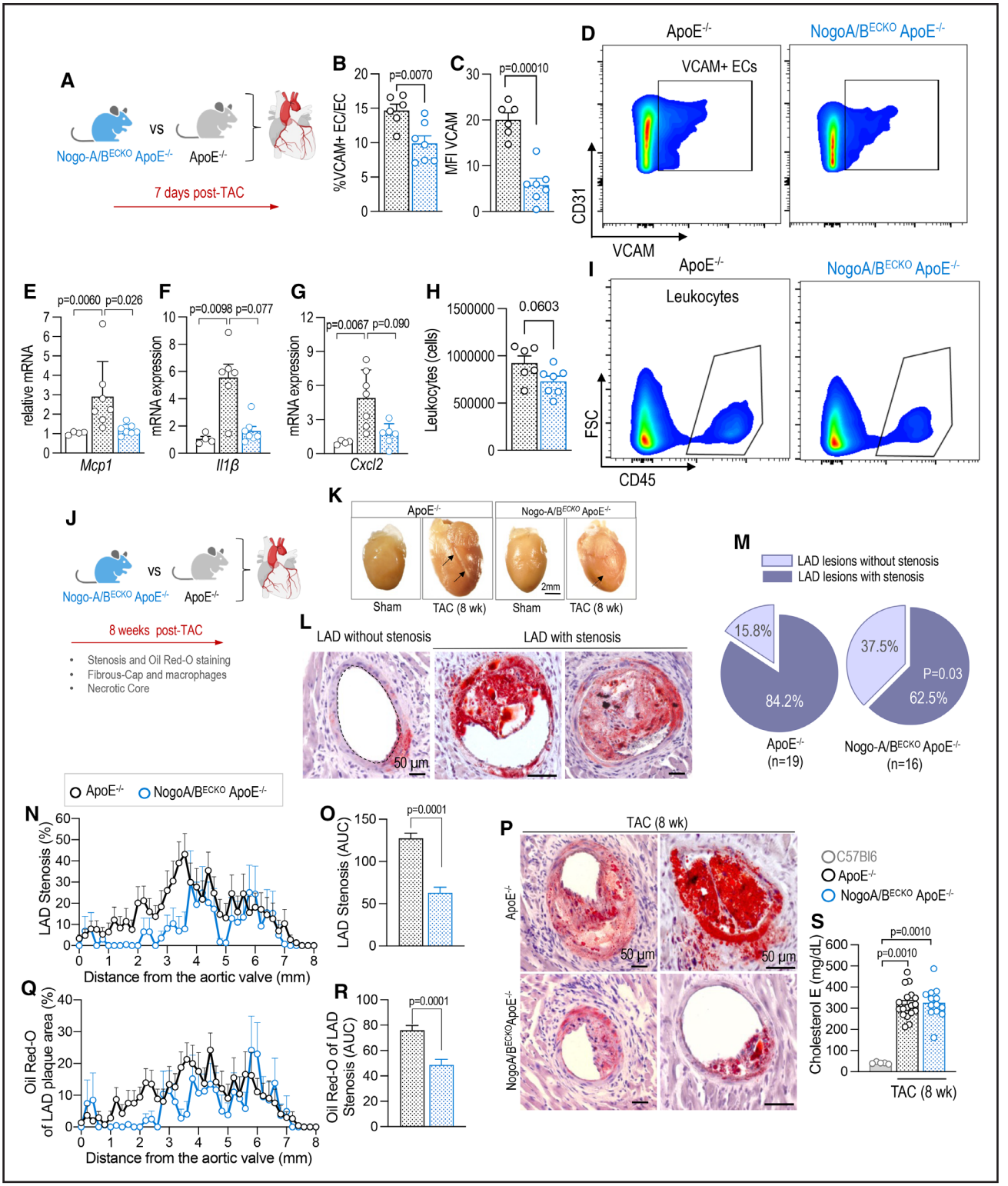


**Figure 2. Endothelial Nogo-B deletion protects the mice from coronary atherosclerosis.**

**A**, Scheme of the experimental model. ApoE$^{-/-}$ mice were crossed with floxed-Nogo-A/B VE-cadherin CRE to delete Nogo-B specifically in endothelial cell (EC; hereafter referred to as Nogo-A/B$^{ECKO}$ApoE$^{-/-}$). Mice floxed-Nogo-A/B VE-cadherin CRE$^{-}$ ApoE$^{-/-}$ were used as control (hereafter referred to as ApoE$^{-/-}$). **B** and **C**, Percentage of VCAM+ EC from the hearts of ApoE$^{-/-}$ (n=6) and Nogo-A/B$^{ECKO}$ApoE$^{-/-}$ (n=7) at 7 days post–transverse aortic constriction (TAC), and (**D**) representative images of VCAM1+ EC FACS (fluorescence-activated cell sorting) analysis plot. Statistical significance was determined by unpaired *t* test (**B** and **C**). **E** through **G**, RTPCR of inflammatory genes in myocardial EC isolated from sham (n=4) or TAC-operated mice (ApoE$^{-/-}$ n=6–7; Nogo-A/B$^{ECKO}$ApoE$^{-/-}$ n=6–7) 3 to 5 days post-surgery. Statistical significance was determined by Kruskal-Wallis followed by Dunn multiple comparison test. **H**, FACS analysis of leukocytes in the hearts of ApoE$^{-/-}$ (n=6) and Nogo-A/B$^{ECKO}$ApoE$^{-/-}$ (n=7) at 7 days post-TAC. Statistical significance was assessed with unpaired *t* test. (*Continued*)

disease in mice. This might be due to a limitation of the mouse model.

## Endothelial NOGO-B Deletion Enhanced Coronary Plaque Stability and Reduced Necrotic Core and Macrophage Infiltration

To investigate the cellular basis of reduced atherosclerosis in Nogo-A/B$^{ECKO}$ApoE$^{-/-}$, we examined 2 commonly used morphological markers of plaque vulnerability, fibrous cap thickness, and necrotic core size.[41] Remarkably, the fibrous cap, evidenced by collagen-I and α-SMA (α-smooth muscle actin) staining, was significantly thicker in Nogo-A/B$^{ECKO}$ApoE$^{-/-}$ mice, (Figure 4A and 4B; Figure S8). This finding was supported by the reduced necrotic core area Nogo-A/B$^{ECKO}$ApoE$^{-/-}$ LAD lesions (Figure 4C and 4D). To further explore the involvement of immune-driven mechanisms, we stained LAD plaques for CD68, a lineage marker of monocyte/macrophage (Figure 4E). Interestingly, CD68+ staining was significantly reduced in Nogo-A/B$^{ECKO}$ApoE$^{-/-}$ compared with ApoE$^{-/-}$ LAD lesions (Figure 4F). Taken together, these findings indicate that the loss of endothelial NOGO-B refrains the progression of atherosclerosis, by decreasing inflammation, necrotic core formation, and plaque vulnerability of coronary lesions.

## Atherosclerosis in the Ascending Aorta and Right Carotid Artery Exposed to High Pressure Were Reduced in the Absence of Endothelial NOGO-B

As in coronary arteries, TAC induces the formation of atherosclerotic lesions in vascular segments exposed to high pressure, like ascending aorta and right carotid artery (Figure 5A).[42] At 8 weeks post-TAC, oil-red-O staining was significantly lower in Nogo-A/B$^{ECKO}$ versus ApoE$^{-/-}$ ascending aorta and right carotid artery (Figure 5B and 5C).

Next, FACS analysis showed that in Nogo-A/B$^{ECKO}$ApoE$^{-/-}$ mice, the total number of macrophages (F4/80+ cells) and monocyte-derived macrophage (CCR2+ cells) in the high-pressured vascular beds was markedly lower compared with ApoE$^{-/-}$ mice (Table 2; Figure 5D through 5F; Figure S9). However, no differences were observed in CD11b+ and CD206+ macrophages (Figure 5G and 5H), respectively pro-[43] and anti-inflammatory.[44] These data suggest that the loss of NOGO-B in EC refrained the inflammatory flux from the bloodstream to the vascular wall without affecting the pro- and anti-inflammatory macrophage populations.

## Endothelial NOGO-B Deletion Sustained the Rewiring of Sphingolipid Metabolism Toward S1P Imparting an Atheroprotective Transcriptional Signature

Measurements of sphingolipids in myocardial EC from mice at 8 weeks post-TAC (Figure 6A) showed a significant increase of dihydrosphingosine (ca. 3.5-fold versus sham, Figure 6B), as well as dihydrosphingosine-1P and dhCer-16:0 (Figure 6C and 6D) suggesting an upregulation of the de novo biosynthesis. Interestingly, total ceramides were not changed in EC from 8 weeks TAC-operated mice versus sham (Figure 6E), whereas sphingosine levels were significantly increased (ca. 2-fold; Figure 6F) suggesting a sustained degradation of ceramide to sphingosine refrained ceramide from accrual. Of note, in addition to ceramide degradation, the recycling pathway could also contribute to sphingosine levels. Nonetheless, these data suggest that ceramide accrual is not implicated in endothelial dysfunction during atherosclerosis. Interestingly, at 8 weeks post-TAC, the upregulation of S1P-ceramide ratio was no longer sustained (Figure 1Q). Next, we compared the sphingolipid levels in myocardial EC, with and without NOGO-B, isolated from mice at 8 weeks post-TAC (Figure 6I). In the absence of NOGO-B, dihydrosphingosine-1P was

**Figure 2 Continued.** **I**, Representative images of CD45+ FACS analysis plots. **J**, Scheme experimental design. At 8 weeks post-TAC, ApoE$^{-/-}$ and Nogo-A/B$^{ECKO}$ApoE$^{-/-}$ left anterior descending (LAD) lesions were analyzed throughout the heart. **K**, Images of hearts from sham and TAC-operated mice at 8 weeks post-surgery. The arrows indicate lipid accumulation (atherosclerotic lesions) in the LAD of ApoE$^{-/-}$, and milder in the LAD of Nogo-A/B$^{ECKO}$ApoE$^{-/-}$ hearts. **L**, Oil-red O/hematoxylin staining show initial lipid accumulation in the intima and some smooth muscle cell (SMC) of the LAD without stenosis (**left**) and images of atherosclerotic lesions of the LAD with marked stenosis (**center** and **right**). **M**, Quantification of the occurrence of LAD lesions without and with stenosis in ApoE$^{-/-}$ and Nogo-A/B$^{ECKO}$ ApoE$^{-/-}$ mice at 8 weeks post-TAC. Statistical significance was assessed by the binomial test, method Wilson/Brown. **N**, Quantification and mapping of the LAD stenosis in 8 weeks TAC-operated ApoE$^{-/-}$ (n=19) and Nogo-A/B$^{ECKO}$ApoE$^{-/-}$ (n=16) mice. Myocardial sections were stained with oil-red-O/hematoxylin, and LAD stenosis was measured throughout the hearts as detailed in Methods. The *x* axis shows the distance from the aortic valve considered as referent point (0 mm) toward the apex. **O**, Bar graph represents the area under the curve of LAD stenosis in both groups. **P**, Representative images of oil-red-O/hematoxylin-stained LAD lesions from ApoE$^{-/-}$ and Nogo-A/B$^{ECKO}$ApoE$^{-/-}$ hearts. **Q**, Quantification of oil-red-O staining expressed as percentage of the plaque area, in 8-week TAC-operated ApoE$^{-/-}$ (n=19) and Nogo-A/B$^{ECKO}$ApoE$^{-/-}$ (n=16) mice. **R**, Bar graph representing the area under the curve of Oil-red-O staining in LAD plaques in both groups. Data are expressed as mean±SEM. Statistical significance was assessed by unpaired *t* test (**O** and **R**). **S**, Cholesterol levels measured in the plasma of C57Bl6 (n=5), ApoE$^{-/-}$ (n=18), and Nogo-A/B$^{ECKO}$ApoE$^{-/-}$ (n=13) mice. Statistical significance was assessed by 1-way ANOVA by Tukey multiple comparison test. (**B**, **C**, **E** through **H**, **O**, **R**, **S**). Data are expressed as mean±SEM. Scale bar, 50 µm. AUC indicates area under the curve; CRE, Cre recombinase; FACS, fluorescence-activated cell sorting; MFI, mean fluorescence intensity; RTPCR, reverse transcription polymerase chain reaction; VCAM, vascular cell adhesion molecule; and VE, vascular endothelial.

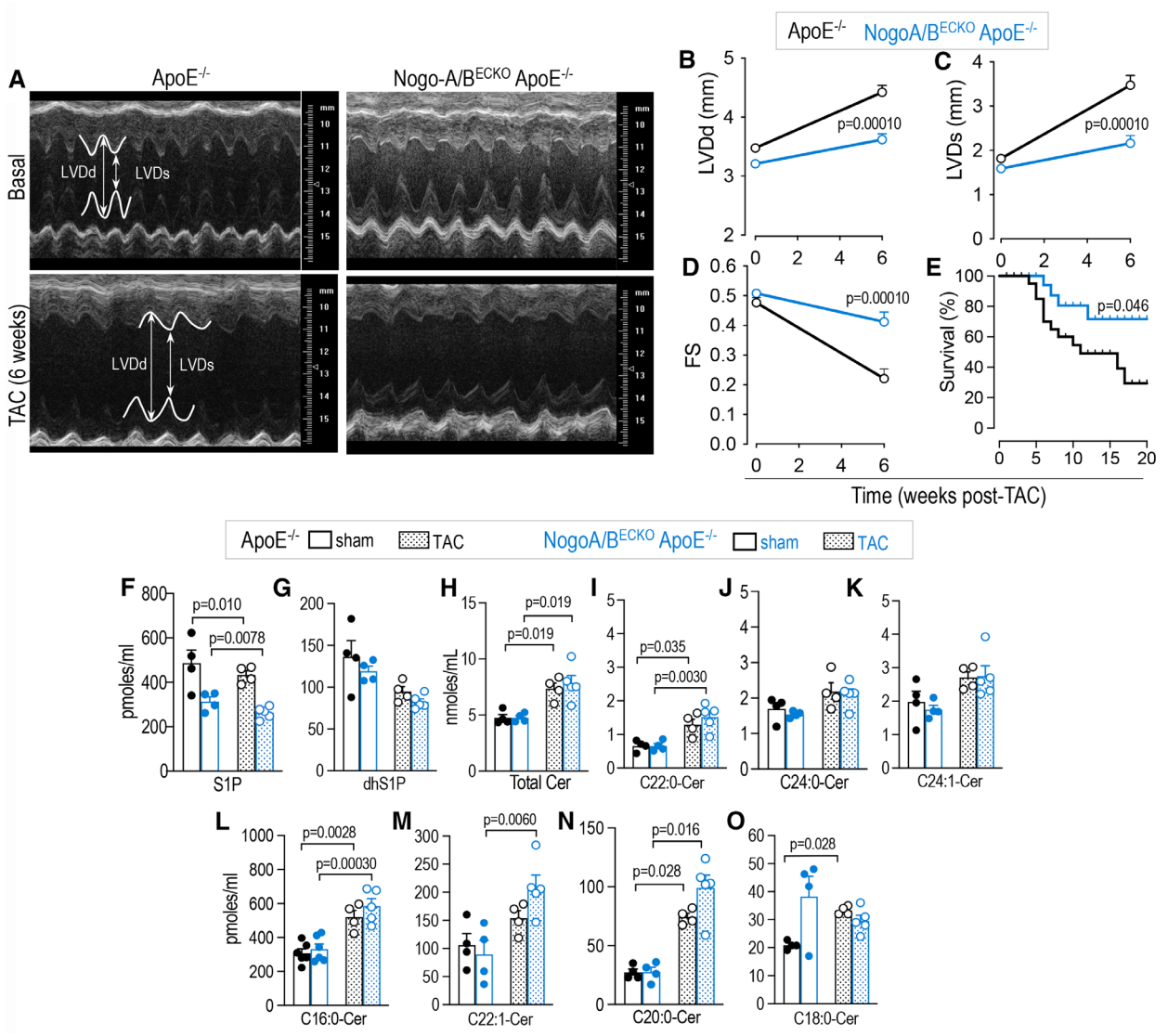


**Figure 3. Cardiac function and survival rate were improved in ApoE$^{-/-}$ mice deleted of endothelial NOGO-B (reticulon-4B).** **A**, Representative images of 2-dimensional guided M-mode echocardiography of the left ventricle (LV) in 8 weeks post–transverse aortic constriction (TAC) and sham of Nogo-A/B$^{ECKO}$ApoE$^{-/-}$ and ApoE$^{-/-}$ mice. Graphs derived from echocardiographic analysis of (**B**) LV end-diastolic diameter (LVDd), (**C**) LV end systolic (LVDs) diameter, and (**D**) fractional shortening (FS). n≥15/group. Statistical significance was determined by 2-way ANOVA followed by Tukey multiple comparison test. **E**, Kaplan-Meier curve showing the percentage of survival of ApoE$^{-/-}$ and Nogo-A/B$^{ECKO}$ApoE$^{-/-}$ mice (n=23/group), at different times post-TAC. Statistical significance was assessed by Gehan-Breslow-Wilcoxon test. Plasma measurements of (**F**) S1P (sphingosine-1-phosphate), (**G**) dhS1P, (**H**) total ceramides, and (**I** through **O**) specific ceramide species at 8 weeks following sham or TAC surgery. Statistical significance was determined by (**F** through **M**) 2-way ANOVA followed by Tukey multiple comparison test, and (**N** and **O**) Mann-Whitney *U* test (**B**–**D**, **F**–**O**). Data are expressed as mean±SEM.

significantly elevated, suggesting an upregulation of the de novo biosynthesis (Figure 6J; Table 2).

Total ceramides were not affected, whereas S1P levels and S1P-ceramide ratio were significantly augmented suggesting a greater ceramide-sphingosine-S1P flux. These data demonstrated that NOGO-B deletion sustained the sphingolipid metabolic rewiring towards S1P over ceramide (Figure 6L and 6K).

To better understand the impact of this metabolic shift on EC phenotype and functions we performed an RNAseq at 8 weeks post-TAC (Figure 6M and 6N). Interestingly, the loss of NOGO-B reduced the expression of proatherosclerotic genes (ie, *Cxcl2, Il1β, Jun and Lpl, Cd36*) while increasing the expression of anti-atherosclerotic genes (ie, *Nr4a1, Abcg1, Nos3, Klf2 and S1pr1*) in myocardial EC (Figure 6M and 6N). Interestingly *Asah1* and *Asah2*, genes codifying for 2 ceramidases, degrading ceramide to sphingosine, were significantly increased in absence of NOGO-B, supporting the enhanced ceramide-sphingosine conversion.

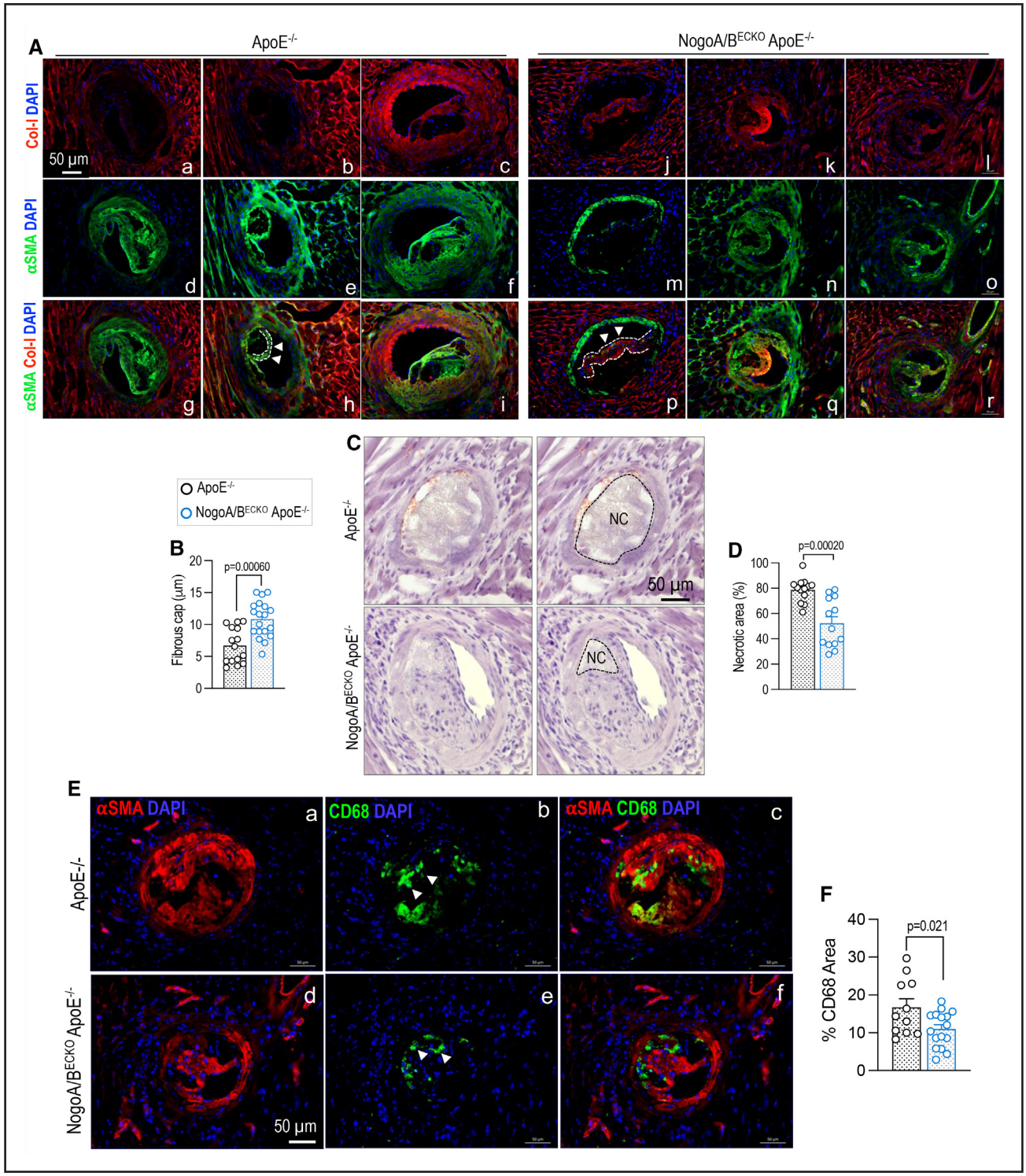


**Figure 4. The loss of endothelial NOGO-B (reticulon-4B) enhanced coronary plaque stability and reduced necrotic core and macrophage infiltration.**

**A**, Immunofluorescent staining of left anterior descending (LAD) lesions for collagen-I, α-SMA (α-smooth muscle actin) (smooth muscle cell [SMC], green) and DAPI (nuclei, blue). Fibrous caps indicated with arrowheads in **Ah** and **Ap**. **B**, Quantification of the fibrous cap thickness in ApoE$^{-/-}$ (LAD plaques=15, n=12 mice) and Nogo-A/B$^{ECKO}$ApoE$^{-/-}$ (LAD plaques=19; n=13 mice) mice at 8 weeks post-TAC. **C**, Representative H&E staining of LAD plaques showing the necrotic core (black dotted lines) and (**D**) quantification in ApoE$^{-/-}$ (LAD plaques=13; n=6 mice) and Nogo-A/B$^{ECKO}$ApoE$^{-/-}$ (LAD lesions=13; n=8 mice) mice at 8 weeks post-TAC. **E**, Representative images of immunofluorescent staining for CD68 (monocyte/macrophage, green) indicated by arrowheads, α-SMA (SMC, red), DAPI (blue) and (**F**) quantification of CD68 area (% of the plaque area) of LAD plaques in ApoE$^{-/-}$ (LAD plaques=11, n=10 mice) and Nogo-A/B$^{ECKO}$ApoE$^{-/-}$ (LAD lesions=16; n=8 mice) mice at 8 weeks post-TAC. Data are expressed as mean±SEM. Statistical significance was determined by (**B**) Mann-Whitney *U* test and (**D** and **F**) unpaired *t* test. Scale bar: 50 μm. ECKO indicates EC knockout.

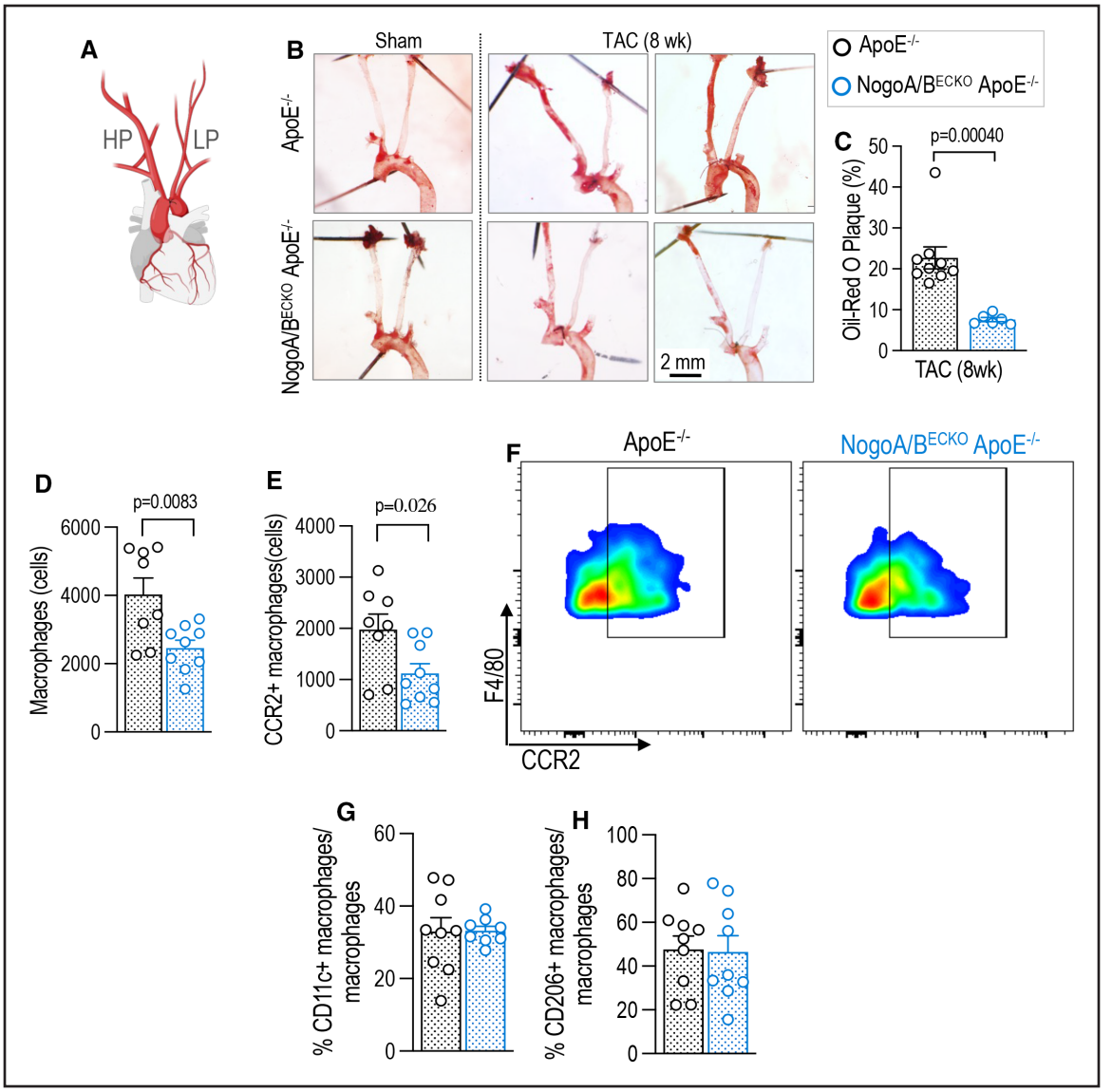


**Figure 5. Endothelial Nogo-B deletion protected the mice from developing atherosclerosis and inflammation in the right carotid artery exposed to high pressure after transverse aortic constriction (TAC).**

**A**, Scheme, after TAC, the right carotid artery is exposed to high pressure (HP) and left carotid artery to low pressure (LP). **B**, Representative images of left and right carotid arteries from ApoE$^{-/-}$ and Nogo-A/B$^{ECKO}$ApoE$^{-/-}$ mice stained with oil red-O at 8 weeks post-TAC. **C**, Quantification of oil red-O staining in the ascending aorta and right carotid artery expressed as percentage of total vessel area in ApoE$^{-/-}$ (n=8 mice) and Nogo-A/B$^{ECKO}$ApoE$^{-/-}$ (n=6 mice). Statistical significance was assessed with Mann-Whitney *U* test. **D** through **H**, At 8 weeks post-TAC, inflammatory cell infiltration of ApoE$^{-/-}$ and Nogo-A/B$^{ECKO}$ApoE$^{-/-}$ right carotid arteries was assessed by FACS (fluorescence-activated cell sorting) analysis, and cells were expressed as number (**D**) or percentage of F4/80+ cells (**E**, **G**, **H**) per right carotid artery. Macrophage populations: (**D**) F4/80+, (**E**) CCR2+ followed by (**F**) representative FACS dop plots. **G**, CD11b+ and (H) CD206+ cells. **D**, **E**, **G**, **H**, Statistical significance was determined by unpaired *t* test. **C** through **E**, **G**, **H**, Data are expressed as mean±SEM. CCR2 indicates C-C chemokine receptor type 2; CD11c, cluster differentiation 11c; and CD206, cluster differentiation 206 (C-type mannose receptor 1).

## DISCUSSION

This is the first study investigating how sphingolipid metabolism and signaling change and impact endothelial dysfunction in a novel model of coronary atherosclerosis in mice. Here, we demonstrated that ceramides are not elevated in myocardial EC isolated from mice with coronary atherosclerosis (Figure 6), which is a paradigm shift from the current belief that ceramide accrual contributes to endothelial dysfunction, mainly deduced by in vitro paradigms.[8] This study identified a heretofore-underappreciated metabolic shift favoring S1P over ceramide in myocardial EC exposed to hemodynamic stress with protective capacity. This change channeled the de novo sphingolipid biosynthesis toward dihydrosphingosine-1P and S1P formation, both bioactive lipids with vasculoprotective capacity. Sustaining this S1P metabolic shift in vivo, by deleting

**Table 2. Absolute Values of Sphingolipid Measurements (Shown in Figure 6J) in Myocardial Endothelial Cells Isolated From ApoE$^{-/-}$ and Nogo-A/B$^{ECKO}$ApoE$^{-/-}$ Mice at 8 Weeks Post-TAC**

| Sphingolipid measurements shown in Figure 6J | | | | | | | | |
|---|---|---|---|---|---|---|---|---|
| ApoE$^{-/-}$ 8 wks post-TAC | | | | | | | | |
| dhCer-16:0 | pmoL/ mg | 27.66 | 24.24 | 33.48 | 21.27 | 21.11 | 24.58 | 29.12 |
| dhSph | pmoL/mg | 74.16 | 73.30 | 73.16 | 71.57 | 70.54 | 73.45 | 68.61 |
| dhSph-1P | pmoL/ mg | 2.93 | 1.86 | 1.33 | 1.97 | 0.80 | 1.15 | 2.00 |
| Sph | pmoL/mg | 133.54 | 155.02 | 162.98 | 147.78 | 153.00 | 156.41 | 150.01 |
| S1P | pmoL/ mg | 0.09 | 0.11 | 0.09 | 0.05 | 0.07 | 0.03 | 0.10 |
| Total Cer | pmoL/mg | 1522.50 | 1662.00 | 1903.50 | 1470.00 | 1461.00 | 1550.00 | 1689.00 |
| S1P/Cer | | $5.60\times10^{-5}$ | $6.84\times10^{-5}$ | $5.60\times10^{-5}$ | $3.11\times10^{-5}$ | $4.35\times10^{-5}$ | $1.87\times10^{-5}$ | $6.22\times10^{-5}$ |
| Total SM | pmoL/mg | 21 939.44 | 21 649 | 22 474.98 | 22 717.22 | 22 505.88 | 20 850.92 | 21 159.25 |
| Nogo-A/B $^{ECKO}$ ApoE$^{-/-}$ 8 wks post-TAC | | | | | | | | |
| dhCer-16:0 | pmoL/ mg | 30.50 | 16.62 | 33.80 | 35.75 | 34.08 | 18.45 | 20.35 |
| dhSph | pmoL/mg | 61.83 | 62.36 | 62.18 | 65.03 | 64.37 | 62.20 | 64.52 |
| dhSph-1P | pmol/ mg | 2.25 | 3.85 | 1.68 | 1.47 | 3.86 | 3.78 | 2.73 |
| Sph | pmol/mg | 135.06 | 122.56 | 123.80 | 143.72 | 144.65 | 139.33 | 129.28 |
| S1P | pmoL/ mg | 0.16 | 0.18 | 0.17 | 0.08 | 0.13 | 0.08 | 0.11 |
| Total Cer | pmoL/mg | 1823.00 | 1364.00 | 1645.00 | 1981.00 | 1784.00 | 1438.00 | 1471.00 |
| S1P/Cer | | $9.73\times10^{-5}$ | $1.10\times10^{-4}$ | $1.03\times10^{-4}$ | $4.87\times10^{-5}$ | $7.91\times10^{-5}$ | $4.87\times10^{-5}$ | $6.69\times10^{-5}$ |
| Total SM | pmoL/mg | 24 889.13 | 21 140.83 | 20 644.35 | 22 995.56 | 21 242.39 | 21 842.18 | 22 760.16 |

dhSph indicates dihydrosphingosine; dhSph-1P, ihydrosphingosine-1-phosphate; S1P, sphingosine-1-phosphate; Sph, sphingosine; and TAC, transverse aortic constriction.

NOGO-B in EC, refrained endothelial activation and coronary atherosclerosis development and progression in ApoE$^{-/-}$ mice. These metabolic changes imparted an anti-atherosclerotic transcriptional signature of EC lacking NOGO-B, supporting reduced coronary atherosclerosis in vivo (graphical abstract).

Our data demonstrated that in mice with coronary atherosclerosis, endothelial sphingolipid de novo biosynthesis is increased (ie, increased dihydrosphingosine and dhCer-16:0), without resulting in ceramide accrual (Figure 6). This is due to both enhanced phosphorylation of dihydrosphingosine and degradation of ceramide to sphingosine, and S1P formation. The outcome of these metabolic changes is the buildup of a vasculoprotective mechanism allowing the EC to shift the S1P-ceramide ratio toward S1P signaling. Another potential mechanism for EC to limit ceramide accrual is via the release of extracellular vesicles, recently proposed as biomarkers for cardiovascular diseases.[45] Elevation of distinct ceramides (e.i. C24:1-cer) in extracellular vesicles was associated with increased risk for major adverse cardiovascular events.[46]

The upregulation of NOGO-B expression in myocardial EC of pressure-overloaded hearts (Figure 1F and 1G) suggested that NOGO-B was counterbalancing this protective mechanism by refraining sphingolipid de novo biosynthesis. Indeed, in vivo data using a genetic approach (ie, Nogo-B deletion in EC) demonstrated that NOGO-B regulation of sphingolipid de novo synthesis contributed to EC activation following hemodynamic stress, leading to the initiation of atherosclerotic events and progressive plaque formation. Metabolically, *Nogo-B* deletion enhanced the de novo biosynthesis (ie, increased dihydrosphingosine-1P) and S1P synthesis, shifting the S1P-ceramide rheostat toward S1P signaling, vasculoprotective. The loss of NOGO-B significantly increased the phosphorylation of both dihydrosphingosine and sphingosine to dihydrosphingosine-1P and S1P respectively (ca. 2-fold), which could explain the slightly lower dihydrosphingosine and sphingosine levels compared with EC replete with NOGO-B. This effect was not due to elevated sphingosine kinase-1 or 2 expressions (data not shown), but likely to the enhanced sphingolipid flux. Interestingly, mRNA levels of *Asah1*[47] and *Asah2*,[48] key enzymes degrading ceramides into sphingosine and free fatty acids, were significantly increased in the absence of NOGO-B, suggesting that ceramides were preferentially degraded to sphingosine and channeled towards S1P. While the mechanism underlying *Asah1* and *Asah2* overexpression in EC lacking Nogo was beyond the scope of this work, a recent study from Wang and colleagues, demonstrated that S1P may be able to upregulate *Asah-1* gene transcription in positive feedback signaling.[49]

Products of sphingosine kinases,[50] both S1P and dihydrosphingosine-1P are bioactive lipids able to activate S1P receptors,[51–53] with plasma dihydrosphingosine-1P levels being ca. 20% to 30% of S1P (Figure 3G), similar to human plasma.[54]

Endothelial-derived S1P plays an important role in cardiovascular homeostasis and is tightly regulated to

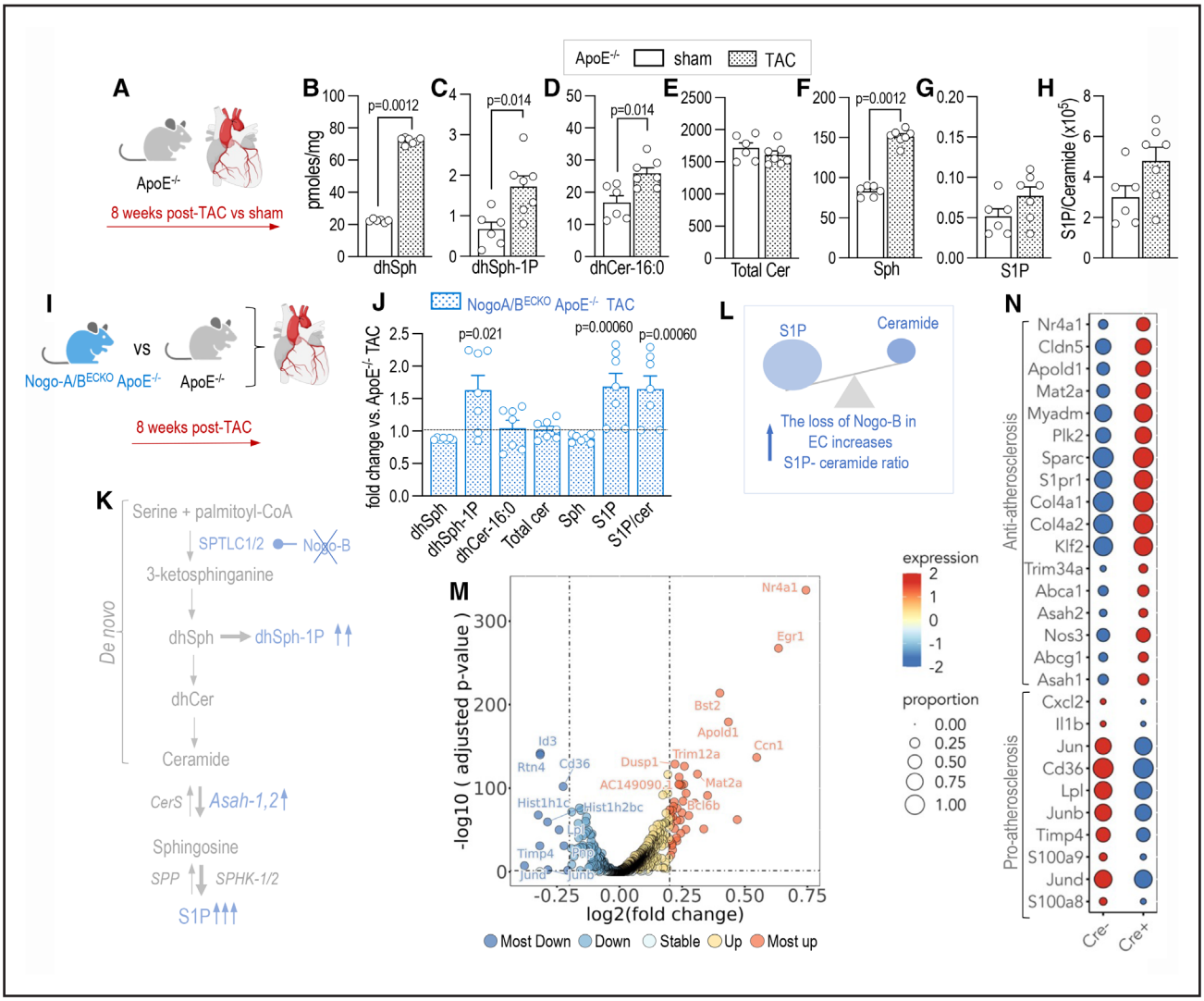


**Figure 6. The loss of NOGO-B suppressed endothelial cell (EC) activation at early and later time points post–transverse aortic constriction (TAC).**

**A**, Scheme ECs were isolated from 8 weeks TAC- (n=7) or sham-operated (n=6) ApoE$^{-/-}$ mice and measured for sphingolipids by LC/MS/MS. **B**, dihydrosphingosine (dhSph), (**C**) dihydrosphingosine-1-phosphate (dhSph-1P), (**D**) dhCer-16:0, (**E**) total ceramides, (**F**) sphingosine (Sph), (**G**) S1P (sphingosine-1-phosphate), and (**H**) S1P/ceramide ratio. **B** through **H**, Statistical significance was assessed by using Mann-Whitney *U* test. **I**, Scheme ECs were isolated from Nogo-A/B$^{ECKO}$ApoE$^{-/-}$ and ApoE$^{-/-}$ at 8 weeks post-TAC for sphingolipid measurement. **J**, Myocardial EC sphingolipids (dhSph, dhSph-1P, dhCer-16:0, total ceramides, Sph, S1P) and S1P/ceramide ratio in Nogo-A/B$^{ECKO}$ApoE$^{-/-}$ EC (n=7) were expressed relative to ApoE$^{-/-}$ EC at 8 weeks post-TAC. Statistical significance was assessed by Kolmogorov-Smirnov test. **K**, Scheme of the de novo sphingolipid pathway indicating major species affected by NOGO-B deletion under prolonged hemodynamic stress. **L**, Changes in S1P/ceramide ratio in EC lacking NOGO-B exposed to prolonged hemodynamic stress. **M**, Volcano plot showing log2-fold of change (*x* axis) and the –log10 *P* value (*y*-axis; upregulated genes are shown in red, $P<0.05$, FC>1; downregulated genes are shown in blue, $P<0.05$, FC<–1) in EC isolated from hearts of ApoE$^{-/-}$ and Nogo-A/B$^{ECKO}$ApoE$^{-/-}$ mice at 8 weeks post-TAC. N=3 mice per group. **N**, Heatmap showing pro- and anti-atherosclerotic genes in FACS (fluorescence-activated cell sorting) sorted EC isolated from hearts of ApoE$^{-/-}$ and Nogo-A/B$^{ECKO}$ApoE$^{-/-}$ mice at 8 weeks post-TAC. Genes are ordered from top to bottom based on log2FC of Cre+ vs Cre–. The color of dot represents the *z* score of log UMI. The sizes of the dots represent the percentage of cells with corresponding gene expression. All genes have Benjamini-Hochberg adjusted $P<0.05$. **B** through **H**, **J**, Data are expressed as mean±SEM. FACS indicates fluorescence-activated cell sorting; MS, mass spectrometry; and LC, liquid chromatography.

maintain several important functions.[8,16,32,55] The deletion of endothelial S1P transporter Spns2 (spinster-2) impaired flow-induced vasodilation, increased blood pressure at baseline, and worsened hypertension and cardiac hypertrophy following chronic infusion of angiotensin-II.[55] S1PR1 is the most abundant S1P receptor in EC and a potent activator of eNOS.[8] Postnatal excision of endothelial S1PR1 or chronic treatment with FTY720, downregulating S1PR1 expression, also disrupted flow-mediated vasodilation and increased blood pressure.[27] Furthermore, Galvani and colleagues elegantly demonstrated that endothelial S1PR1 had atheroprotective functions in mice,[29] in part due to inhibition of NF-kB (nuclear factor kappa B) signaling.

We reported that deletion of endothelial NOGO-B enhanced S1P production and S1PR1 signaling, resulting in resistance to hypertension mainly due to elevated eNOS-derived NO production,[32] and reduced inflammation ascribed to heightened endothelial barrier function,[30,31] all mechanisms supporting the atheroprotective phenotype of Nogo-A/B$^{ECKO}$ApoE$^{-/-}$ mice.

In this study, we demonstrated that myocardial EC lacking NOGO-B were resistant to activation following hemodynamic stress at an early time point (7 days), as shown by reduced VCAM1 and inflammatory gene expression (ie, *Mcp1, Il1β,* and *Cxcl2)*. VCAM1 was suggested to play a major role in the initiation of atherosclerosis,[39] while clinical and preclinical studies underlined the key role of IL1β in atherosclerosis development and progression.[56,57] In line with reduced EC activation, coronary and carotid lesions of Nogo-A/B$^{ECKO}$ApoE$^{-/-}$ mice had reduced number of macrophages, suggesting a lower recruitment due not only to the lower levels of VCAM, and cytokines/chemokines, but most likely also to enhanced S1P-mediated barrier function,[30,31] as previously reported. Furthermore, deletion of endothelial NOGO-B increased plaque stability as shown by higher fibrous cap thickness and reduced necrotic core size (Figure 4).

Interestingly, RNAseq data on EC isolated from mice affected by coronary lesions (8 weeks post-TAC) showed a remarkable atheroprotective gene profile when NOGO-B was deleted (Figure 6). The loss of NOGO-B significantly increased the expression of *S1pr1*, which increases the barrier function, eNOS-derived NO formation, and suppresses inflammation.[8,27,58] Furthermore, a recent study from Akhter and colleagues showed that in a mouse model of endotoxemia S1P generation induced the programming of S1PR1$^{low}$ to S1PR$^{high}$ aiding the reestablishment of endothelial barrier.[59] Thus, it is possible that in absence of NOGO-B, endothelial-derived S1P drives this positive feedback enhancing *Spr1* expression and endothelial function.

*Abcg1 and Abca1* upregulated in EC lacking NOGO-B, have been shown to protect mice from atherosclerosis.[60] *Col4a1 and Col4a2* genes were increased by *Nogo-B* deletion supporting the thicker fibrous cap and more stable plaques. Interestingly, human variants of Col4a1 and Col4a2 have been associated with plaque vulnerability.[61] On the contrary, many proatherosclerotic genes were significantly reduced in absence of NOGO-B (ie, *Cxcl2, Il1b, Jun, Cd36*, etc). A large body of literature linked the hemodynamic disturbance with transcriptional regulation of functional phenotype in EC.[3] High expression of Kruppel-like factor 2 (*Klf2*), considered the most responsive transcriptional factor to flow, has been shown in EC of atheroresistent regions in humans.[62] KLF2 promotes an anti-inflammatory and antithrombotic endothelial phenotype, by suppressing NF-kB, and upregulating *nos3*[63] and *S1pr1*,[64] among other genes.[3] Hence, in the absence of NOGO-B, the increased expression of *nos3* and *S1pr1* in EC could be also due to *klf2* upregulation. It is noteworthy to underline that S1P-S1PR1 signaling is a key player in flow-mediated vasodilation[16,55] and endothelial response to shear stress, including alignment, signaling, and vascular development.[65]

One limitation of our study is the use of myocardial EC instead of coronary EC to overcome the insufficient cell number for the different analyses performed.

In summary, using a model of coronary atherosclerosis in ApoE$^{-/-}$ mice, we demonstrated a rewiring of sphingolipid metabolism toward S1P and dihydrosphingosine-1P in EC exposed to hemodynamic stress, which is transient and protective. The deletion of NOGO-B can enhance and sustain the rewiring of sphingolipid metabolism towards S1P and its atheroprotective capacity. Our findings also disprove the increase of ceramides as a mechanism contributing to endothelial dysfunction in atherosclerosis and set forth the foundation for sphingolipid-based therapeutics to limit atheroprogression.

## ARTICLE INFORMATION

Received October 11, 2023; revision received February 13, 2024; accepted February 26, 2024.

### Affiliations

Department of Pathology and Laboratory Medicine, Cardiovascular Research Institute, Brain and Mind Research Institute (O.L.M., J.N., L.S., A.M., L.R., S.P., A.B., A.D.L.) and Department of Physiology and Biophysics, Institute for Computational Biomedicine (Y.H., O.E.), Weill Cornell Medicine, New York. Department of Excellence of Pharmacological and Biomolecular Sciences, University of Milan, Milano, Italy (J.N., G.D.N.). Pôle de Recherche Cardiovasculaire, Institut de Recherche Expérimentale et Clinique, Université catholique de Louvain, Brussels, Belgium (A.M.). Department of Pharmacy, School of Medicine, University of Naples Federico II, Italy (M.S., M.R.B.). Department of Anesthesiology, Medical College of Wisconsin Cardiovascular Center, Medical College of Wisconsin, Milwaukee (J.K.F.).

### Sources of Funding

This work was supported by National Institutes of Health grant R01HL126913, R01HL 152195 and a Harold S. Geneen Charitable Trust Award for Coronary Heart Disease Research to A. Di Lorenzo.

### Disclosures

None.

### Supplemental Material

Figures S1–S9
References 16,36–41

## REFERENCES

1. Gimbrone MA Jr, García-Cardeña G. Vascular endothelium, hemodynamics, and the pathobiology of atherosclerosis. *Cardiovasc Pathol*. 2013;22:9–15. doi: 10.1016/j.carpath.2012.06.006
2. Hadi HA, Carr CS, Al Suwaidi J. Endothelial dysfunction: cardiovascular risk factors, therapy, and outcome. *Vasc Health Risk Manag*. 2005;1:183–198. PMID: 17319104
3. Gimbrone MA Jr, García-Cardeña G. Endothelial cell dysfunction and the pathobiology of atherosclerosis. *Circ Res*. 2016;118:620–636. doi: 10.1161/CIRCRESAHA.115.306301
4. Tabas I, Williams KJ, Boren J. Subendothelial lipoprotein retention as the initiating process in atherosclerosis: update and therapeutic implications. *Circulation*. 2007;116:1832–1844. doi: 10.1161/CIRCULATIONAHA.106.676890
5. Pober JS, Sessa WC. Evolving functions of endothelial cells in inflammation. *Nat Rev Immunol*. 2007;7:803–815. doi: 10.1038/nri2171

6. Grundy SM, Stone NJ, Bailey AL, Beam C, Birtcher KK, Blumenthal RS, Braun LT, de Ferranti S, Faiella-Tommasino J, Forman DE, et al. 2018 AHA/ACC/AACVPR/AAPA/ABC/ACPM/ADA/AGS/APhA/ASPC/NLA/PCNA guideline on the management of blood cholesterol: a report of the American college of cardiology/American heart association task force on clinical practice guidelines. *Circulation*. 2019;139:e1082–e1143. doi: 10.1161/CIR.0000000000000625
7. Mach F, Baigent C, Catapano AL, Koskinas KC, Casula M, Badimon L, Chapman MJ, De Backer GG, Delgado V, Ference BA, et al. 2019 ESC/EAS Guidelines for the management of dyslipidaemias: lipid modification to reduce cardiovascular risk. *Eur Heart J*. 2020;41:111–188. doi: 10.1093/eurheartj/ehz455
8. Sasset L, Di Lorenzo A. Sphingolipid metabolism and signaling in endothelial cell functions. *Adv Exp Med Biol*. 2022;1372:87–117. doi: 10.1007/978-981-19-0394-6_8
9. Meeusen JW, Donato LJ, Kopecky SL, Vasile VC, Jaffe AS, Laaksonen R. Ceramides improve atherosclerotic cardiovascular disease risk assessment beyond standard risk factors. *Clin Chim Acta*. 2020;511:138–142. doi: 10.1016/j.cca.2020.10.005
10. Laaksonen R, Ekroos K, Sysi-Aho M, Hilvo M, Vihervaara T, Kauhanen D, Suoniemi M, Hurme R, Marz W, Scharnagl H, et al. Plasma ceramides predict cardiovascular death in patients with stable coronary artery disease and acute coronary syndromes beyond LDL-cholesterol. *Eur Heart J*. 2016;37:1967–1976. doi: 10.1093/eurheartj/ehw148
11. Anroedh S, Hilvo M, Akkerhuis KM, Kauhanen D, Koistinen K, Oemrawsingh R, Serruys P, van Geuns RJ, Boersma E, Laaksonen R, et al. Plasma concentrations of molecular lipid species predict long-term clinical outcome in coronary artery disease patients. *J Lipid Res*. 2018;59:1729–1737. doi: 10.1194/jlr.P081281
12. Poss AM, Maschek JA, Cox JE, Hauner BJ, Hopkins PN, Hunt SC, Holland WL, Summers SA, Playdon MC. Machine learning reveals serum sphingolipids as cholesterol-independent biomarkers of coronary artery disease. *J Clin Invest*. 2020;130:1363–1376. doi: 10.1172/JCI131838
13. Sattler K, Lehmann I, Graler M, Brocker-Preuss M, Erbel R, Heusch G, Levkau B. HDL-bound sphingosine 1-phosphate (S1P) predicts the severity of coronary artery atherosclerosis. *Cell Physiol Biochem*. 2014;34:172–184. doi: 10.1159/000362993
14. Levkau B. HDL-S1P: cardiovascular functions, disease-associated alterations, and therapeutic applications. *Front Pharmacol*. 2015;6:243. doi: 10.3389/fphar.2015.00243
15. Choi RH, Tatum SM, Symons JD, Summers SA, Holland WL. Ceramides and other sphingolipids as drivers of cardiovascular disease. *Nat Rev Cardiol*. 2021;18:701–711. doi: 10.1038/s41569-021-00536-1
16. Cantalupo A, Sasset L, Gargiulo A, Rubinelli L, Del Gaudio I, Benvenuto D, Wadsack C, Jiang XC, Bucci MR, Di Lorenzo A. Endothelial sphingolipid de novo synthesis controls blood pressure by regulating signal transduction and no via ceramide. *Hypertension*. 2020;75:1279–1288. doi: 10.1161/HYPERTENSIONAHA.119.14507
17. Tsuchida T, Murata S, Hasegawa S, Mikami S, Enosawa S, Hsu HC, Fukuda A, Okamoto S, Mori A, Matsuo M, et al. Investigation of clinical safety of human iPS cell-derived liver organoid transplantation to infantile patients in porcine model. *Cell Transplant*. 2020;29:963689720964384. doi: 10.1177/0963689720964384
18. Zhang QJ, Holland WL, Wilson L, Tanner JM, Kearns D, Cahoon JM, Pettey D, Losee J, Duncan B, Gale D, et al. Ceramide mediates vascular dysfunction in diet-induced obesity by PP2A-mediated dephosphorylation of the eNOS-Akt complex. *Diabetes*. 2012;61:1848–1859. doi: 10.2337/db11-1399
19. Li H, Junk P, Huwiler A, Burkhardt C, Wallerath T, Pfeilschifter J, Forstermann U. Dual effect of ceramide on human endothelial cells: induction of oxidative stress and transcriptional upregulation of endothelial nitric oxide synthase. *Circulation*. 2002;106:2250–2256. doi: 10.1161/01.cir.0000035650.05921.50
20. Edsfeldt A, Duner P, Stahlman M, Mollet IG, Asciutto G, Grufman H, Nitulescu M, Persson AF, Fisher RM, Melander O, et al. Sphingolipids contribute to human atherosclerotic plaque inflammation. *Arterioscler Thromb Vasc Biol*. 2016;36:1132–1140. doi: 10.1161/ATVBAHA.116.305675
21. Hojjati MR, Li Z, Jiang XC. Serine palmitoyl-CoA transferase (SPT) deficiency and sphingolipid levels in mice. *Biochim Biophys Acta*. 2005;1737:44–51. doi: 10.1016/j.bbalip.2005.08.006
22. Lee SY, Kim JR, Hu Y, Khan R, Kim SJ, Bharadwaj KG, Davidson MM, Choi CS, Shin KO, Lee YM, et al. Cardiomyocyte specific deficiency of serine palmitoyltransferase subunit 2 reduces ceramide but leads to cardiac dysfunction. *J Biol Chem*. 2012;287:18429–18439. doi: 10.1074/jbc.M111.296947
23. Hojjati MR, Li Z, Zhou H, Tang S, Huan C, Ooi E, Lu S, Jiang XC. Effect of myriocin on plasma sphingolipid metabolism and atherosclerosis in apoE-deficient mice. *J Biol Chem*. 2005;280:10284–10289. doi: 10.1074/jbc.M412348200
24. Park TS, Rosebury W, Kindt EK, Kowala MC, Panek RL. Serine palmitoyltransferase inhibitor myriocin induces the regression of atherosclerotic plaques in hyperlipidemic ApoE-deficient mice. *Pharmacol Res*. 2008;58:45–51. doi: 10.1016/j.phrs.2008.06.005
25. Miyake Y, Kozutsumi Y, Nakamura S, Fujita T, Kawasaki T. Serine palmitoyltransferase is the primary target of a sphingosine-like immunosuppressant, ISP-1/myriocin. *Biochem Biophys Res Commun*. 1995;211:396–403. doi: 10.1006/bbrc.1995.1827
26. Tabas I. Sphingolipids and atherosclerosis: a mechanistic connection? A therapeutic opportunity? *Circulation*. 2004;110:3400–3401. doi: 10.1161/01.CIR.0000150861.98087.56
27. Cantalupo A, Gargiulo A, Dautaj E, Liu C, Zhang Y, Hla T, Di Lorenzo A. S1PR1 (Sphingosine-1-Phosphate Receptor 1) signaling regulates blood flow and pressure. *Hypertension*. 2017;70:426–434. doi: 10.1161/HYPERTENSIONAHA.117.09088
28. Sasset L, Chowdhury KH, Manzo OL, Rubinelli L, Konrad C, Maschek JA, Manfredi G, Holland WL, Di Lorenzo A. Sphingosine-1-phosphate controls endothelial sphingolipid homeostasis via ORMDL. *EMBO Rep*. 2023;24:e54689. doi: 10.15252/embr.202254689
29. Galvani S, Sanson M, Blaho VA, Swendeman SL, Obinata H, Conger H, Dahlback B, Kono M, Proia RL, Smith JD, et al. HDL-bound sphingosine 1-phosphate acts as a biased agonist for the endothelial cell receptor S1P1 to limit vascular inflammation. *Sci Signal*. 2015;8:ra79. doi: 10.1126/scisignal.aaa2581
30. Di Lorenzo A, Manes TD, Davalos A, Wright PL, Sessa WC. Endothelial reticulon-4B (Nogo-B) regulates ICAM-1-mediated leukocyte transmigration and acute inflammation. *Blood*. 2011;117:2284–2295. doi: 10.1182/blood-2010-04-281956
31. Zhang Y, Huang Y, Cantalupo A, Azevedo PS, Siragusa M, Bielawski J, Giordano FJ, Di Lorenzo A. Endothelial Nogo-B regulates sphingolipid biosynthesis to promote pathological cardiac hypertrophy during chronic pressure overload. *JCI Insight*. 2016;1:e85484. doi: 10.1172/jci.insight.85484
32. Cantalupo A, Zhang Y, Kothiya M, Galvani S, Obinata H, Bucci M, Giordano FJ, Jiang XC, Hla T, Di Lorenzo A. Nogo-B regulates endothelial sphingolipid homeostasis to control vascular function and blood pressure. *Nat Med*. 2015;21:1028–1037. doi: 10.1038/nm.3934
33. Domarkiene I, Pranculis A, Germanas S, Jakaitiene A, Vitkus D, Dzenkeviciute V, Kucinskiene Z, Kucinskas V. RTN4 and FBXL17 genes are associated with coronary heart disease in genome-wide association analysis of lithuanian families. *Balkan J Med Genet*. 2013;16:17–22. doi: 10.2478/bjmg-2013-0026
34. Lee WS, Kim SW, Hong SA, Lee TJ, Park ES, Kim HJ, Lee KJ, Kim TH, Kim CJ, Ryu WS. Atherosclerotic progression attenuates the expression of Nogo-B in autopsied coronary artery: pathology and virtual histology intravascular ultrasound analysis. *J Korean Med Sci*. 2009;24:596–604. doi: 10.3346/jkms.2009.24.4.596
35. Rodriguez-Feo JA, Hellings WE, Verhoeven BA, Moll FL, de Kleijn DP, Prendergast J, Gao Y, van der Graaf Y, Tellides G, Sessa WC, et al. Low levels of Nogo-B in human carotid atherosclerotic plaques are associated with an atheromatous phenotype, restenosis, and stenosis severity. *Arterioscler Thromb Vasc Biol*. 2007;27:1354–1360. doi: 10.1161/ATVBAHA.107.140913
36. Marino A, Zhang Y, Rubinelli L, Riemma MA, Ip JE, Di Lorenzo A. Pressure overload leads to coronary plaque formation, progression, and myocardial events in ApoE-/- mice. *JCI Insight*. 2019;4:e128220. doi: 10.1172/jci.insight.128220
37. Acevedo L, Yu J, Erdjument-Bromage H, Miao RQ, Kim JE, Fulton D, Tempst P, Strittmatter SM, Sessa WC. A new role for Nogo as a regulator of vascular remodeling. *Nat Med*. 2004;10:382–388. doi: 10.1038/nm1020
38. Cybulsky MI, Gimbrone MA Jr. Endothelial expression of a mononuclear leukocyte adhesion molecule during atherogenesis. *Science*. 1991;251:788–791. doi: 10.1126/science.1990440
39. Cybulsky MI, Iiyama K, Li H, Zhu S, Chen M, Iiyama M, Davis V, Gutierrez-Ramos JC, Connelly PW, Milstone DS. A major role for VCAM-1, but not ICAM-1, in early atherosclerosis. *J Clin Invest*. 2001;107:1255–1262. doi: 10.1172/JCI11871
40. Weber C, Noels HA. Current pathogenesis and therapeutic options. *Nat Med*. 2011;17:1410–1422. doi: 10.1038/nm.2538
41. Hansson GK, Libby P, Tabas I. Inflammation and plaque vulnerability. *J Intern Med*. 2015;278:483–493. doi: 10.1111/joim.12406
42. Liu D, Lei L, Desir M, Huang Y, Cleman J, Jiang W, Fernandez-Hernando C, Di Lorenzo A, Sessa WC, Giordano FJ. Smooth muscle hypoxia-inducible factor 1alpha links intravascular pressure and

atherosclerosis--brief report. *Arterioscler Thromb Vasc Biol*. 2016;36:442–445. doi: 10.1161/ATVBAHA.115.306861
43. Edsfeldt A, Swart M, Singh P, Dib L, Sun J, Cole JE, Park I, Al-Sharify D, Persson A, Nitulescu M, et al. Interferon regulatory factor-5-dependent CD11c+ macrophages contribute to the formation of rupture-prone atherosclerotic plaques. *Eur Heart J*. 2022;43:1864–1877. doi: 10.1093/eurheartj/ehab920
44. Colin S, Chinetti-Gbaguidi G, Staels B. Macrophage phenotypes in atherosclerosis. *Immunol Rev*. 2014;262:153–166. doi: 10.1111/imr.12218
45. Boulanger CM, Loyer X, Rautou PE, Amabile N. Extracellular vesicles in coronary artery disease. *Nat Rev Cardiol*. 2017;14:259–272. doi: 10.1038/nrcardio.2017.7
46. Timmerman N, Waissi F, Dekker M, de Borst GJ, van Bennekom J, de Winter RJ, Hilvo M, Jylha A, Pasterkamp G, de Kleijn DPV, et al. Ceramides and phospholipids in plasma extracellular vesicles are associated with high risk of major cardiovascular events after carotid endarterectomy. *Sci Rep*. 2022;12:5521. doi: 10.1038/s41598-022-09225-6
47. Bernardo K, Hurwitz R, Zenk T, Desnick RJ, Ferlinz K, Schuchman EH, Sandhoff K. Purification, characterization, and biosynthesis of human acid ceramidase. *J Biol Chem*. 1995;270:11098–11102. doi: 10.1074/jbc.270.19.11098
48. El Bawab S, Bielawska A, Hannun YA. Purification and characterization of a membrane-bound nonlysosomal ceramidase from rat brain. *J Biol Chem*. 1999;274:27948–27955. doi: 10.1074/jbc.274.39.27948
49. Wang W, Sherry T, Cheng X, Fan Q, Cornell R, Liu J, Xiao Z, Pocock R. An intestinal sphingolipid confers intergenerational neuroprotection. *Nat Cell Biol*. 2023;25:1196–1207. doi: 10.1038/s41556-023-01195-9
50. Liu H, Sugiura M, Nava VE, Edsall LC, Kono K, Poulton S, Milstien S, Kohama T, Spiegel S. Molecular cloning and functional characterization of a novel mammalian sphingosine kinase type 2 isoform. *J Biol Chem*. 2000;275:19513–19520. doi: 10.1074/jbc.M002759200
51. Mendelson K, Evans T, Hla T. Sphingosine 1-phosphate signalling. *Development*. 2014;141:5–9. doi: 10.1242/dev.094805
52. Van Brocklyn JR, Tu Z, Edsall LC, Schmidt RR, Spiegel S. Sphingosine 1-phosphate-induced cell rounding and neurite retraction are mediated by the G protein-coupled receptor H218. *J Biol Chem*. 1999;274:4626–4632. doi: 10.1074/jbc.274.8.4626
53. Jin Y, Knudsen E, Wang L, Bryceson Y, Damaj B, Gessani S, Maghazachi AA. Sphingosine 1-phosphate is a novel inhibitor of T-cell proliferation. *Blood*. 2003;101:4909–4915. doi: 10.1182/blood-2002-09-2962
54. Ohkawa R, Nakamura K, Okubo S, Hosogaya S, Ozaki Y, Tozuka M, Osima N, Yokota H, Ikeda H, Yatomi Y. Plasma sphingosine-1-phosphate measurement in healthy subjects: close correlation with red blood cell parameters. *Ann Clin Biochem*. 2008;45:356–363. doi: 10.1258/acb.2007.007189
55. Del Gaudio I, Rubinelli L, Sasset L, Wadsack C, Hla T, Di Lorenzo A. Endothelial Spns2 and ApoM regulation of vascular tone and hypertension via sphingosine-1-phosphate. *J Am Heart Assoc*. 2021;10:e021261. doi: 10.1161/JAHA.121.021261
56. Libby P. Interleukin-1 beta as a target for atherosclerosis therapy: biological basis of CANTOS and beyond. *J Am Coll Cardiol*. 2017;70:2278–2289. doi: 10.1016/j.jacc.2017.09.028
57. Abbate A, Toldo S, Marchetti C, Kron J, Van Tassell BW, Dinarello CA. Interleukin-1 and the inflammasome as therapeutic targets in cardiovascular disease. *Circ Res*. 2020;126:1260–1280. doi: 10.1161/CIRCRESAHA.120.315937
58. Christensen PM, Liu CH, Swendeman SL, Obinata H, Qvortrup K, Nielsen LB, Hla T, Di Lorenzo A, Christoffersen C. Impaired endothelial barrier function in apolipoprotein M-deficient mice is dependent on sphingosine-1-phosphate receptor 1. *FASEB J*. 2016;30:2351–2359. doi: 10.1096/fj.201500064
59. Akhter MZ, Chandra Joshi J, Balaji Ragunathrao VA, Maienschein-Cline M, Proia RL, Malik AB, Mehta D. Programming to S1PR1(+) endothelial cells promotes restoration of vascular integrity. *Circ Res*. 2021;129:221–236. doi: 10.1161/CIRCRESAHA.120.318412
60. Westerterp M, Tsuchiya K, Tattersall IW, Fotakis P, Bochem AE, Molusky MM, Ntonga V, Abramowicz S, Parks JS, Welch CL, et al. Deficiency of ATP-binding cassette transporters A1 and G1 in endothelial cells accelerates atherosclerosis in mice. *Arterioscler Thromb Vasc Biol*. 2016;36:1328–1337. doi: 10.1161/ATVBAHA.115.306670
61. Yang W, Ng FL, Chan K, Pu X, Poston RN, Ren M, An W, Zhang R, Wu J, Yan S, et al. Coronary-heart-disease-associated genetic variant at the COL4A1/COL4A2 locus affects COL4A1/COL4A2 expression, vascular cell survival, atherosclerotic plaque stability and risk of myocardial infarction. *PLoS Genet*. 2016;12:e1006127.
62. Parmar KM, Larman HB, Dai G, Zhang Y, Wang ET, Moorthy SN, Kratz JR, Lin Z, Jain MK, Gimbrone MA Jr, et al. Integration of flow-dependent endothelial phenotypes by Kruppel-like factor 2. *J Clin Invest*. 2006;116:49–58. doi: 10.1172/JCI24787
63. Dekker RJ, van Thienen JV, Rohlena J, de Jager SC, Elderkamp YW, Seppen J, de Vries CJ, Biessen EA, van Berkel TJ, Pannekoek H, et al. Endothelial KLF2 links local arterial shear stress levels to the expression of vascular tone-regulating genes. *Am J Pathol*. 2005;167:609–618. doi: 10.1016/S0002-9440(10)63002-7
64. Sun X, Mathew B, Sammani S, Jacobson JR, Garcia JGN. Simvastatin-induced sphingosine 1-phosphate receptor 1 expression is KLF2-dependent in human lung endothelial cells. *Pulm Circ*. 2017;7:117–125. doi: 10.1177/2045893217701162
65. Jung B, Obinata H, Galvani S, Mendelson K, Ding BS, Skoura A, Kinzel B, Brinkmann V, Rafii S, Evans T, et al. Flow-regulated endothelial S1P receptor-1 signaling sustains vascular development. *Dev Cell*. 2012;23:600–610. doi: 10.1016/j.devcel.2012.07.015